12-2021

Facile Nitrogen-Doping of Screen-Printed Carbon Electrodes for Detection of Hydrogen Peroxide

Emmanuel Nkyaagye
East Tennessee State University

Facile Nitrogen-Doping of Screen-Printed Carbon Electrodes for Detection of Hydrogen Peroxide

---

A thesis

presented to

the faculty of the Department of Chemistry

East Tennessee State University

In partial fulfillment

of the requirements for the degree

Master of Science in Chemistry

---

by

Emmanuel Nkyaagye

December 2021

Dr. Gregory W. Bishop, Chair

Dr. Dane W. Scott

Dr. Catherine McCusker

Dr. Hua Mei

Keywords: nitrogen doping, electrocatalysis, screen printed electrodes, hydrogen peroxide

ABSTRACT

Facile Nitrogen-Doping of Screen-Printed Carbon Electrodes for Detection of Hydrogen Peroxide

by

Emmanuel Nkyaagye

Screen-printed carbon electrodes (SPCEs) have garnered much attention as sensors due to their simplicity and relatively low cost. However, to impart necessary selectivity and sensitivity for specific applications, modification of the SPCE surface, which can involve time-consuming procedures or costly equipment/materials, is typically required. Here, a simple nitrogen-doping process based on NH_4OH was used to modify SPCEs prepared from commercially available ink for electrochemical detection of H_2O_2, a common target for biosensing strategies and indicator of cell stress. XPS studies showed that NH_4OH treatment of SPCEs led to a nearly 5-fold increase in surface nitrogen content (from 0.28% to 1.34%). Compared to SPCEs, nitrogen-doped SPCEs (N-SPCEs) demonstrated enhanced current and lower onset potentials for H_2O_2 reduction. Amperometric detection of H_2O_2 at an applied potential of -0.4 V (vs. Ag/AgCl) using N-SPCEs also exhibited a wider linear range, lower detection limit, and higher sensitivity than SPCEs.

DEDICATION

I dedicate this work to the Department of Chemistry, East Tennessee State University.

ACKNOWLEDGMENTS

I gratefully acknowledge my debt to these wonderful people whose encouragement, assistance, patience, and love led to the completion of this work.

To Dr. Gregory W. Bishop, my supervisor, who supported me with much patience throughout my studies and research.

To Dr. Dane W. Scott, Dr. Catherine McCusker, and Dr. Hua Mei who accepted to serve on my committee and contributed immensely to the completion of this program

To the entire Faculty and Staff of the Department of Chemistry, East Tennessee State University for the great opportunity and aid throughout my study.

To Mr. Thomas Odamtten and my Family for their support, sacrifices, love, and care.

To Dr. Francis Nsiah, I appreciate your kindness and support.

To Ivy Antwi, Eric Wornyo and Emmanuel Peprah Yamoah, my lab colleagues for their support and assistance.

To Dr Xu Feng and Elisha for your contribution.

TABLE OF CONTENTS

LIST OF TABLES

LIST OF FIGURES

LIST OF ABBREVIATIONS

AuNPs	Gold nanoparticles
CNT	Carbon nanotubes
CV	Cyclic Voltammetry
DFT	Density Functional Theory
EP	Electrostatic potential
GrNR	Graphene nanoribbon
HRP	Horseradish peroxidase
N-SPCEs	Nitrogen-doped screen-printed electrode
PBS	Phosphate buffer saline
PPy	Polypyrrole
rGO	Reduced graphene oxide
ROS	Reactive oxygen species
SPCEs	Screen printed carbon electrodes
UMEs	Ultramicroelectrodes

CHAPTER 1. INTRODUCTION

Why Hydrogen Peroxide Detection?

Hydrogen peroxide (H_2O_2) is a non-radical reactive oxygen species (ROS) and common aerobic metabolite. It can diffuse through cell membranes and act as an intercellular and intracellular messenger and a significant antimicrobial agent.[1,2] H_2O_2 responds to extracellular stimuli (for example, insulin) as a redox signaling molecule. Under normal physiological conditions, the concentration of H_2O_2 ranges from approximately 1 to 10 nM in cells.[3] However, under oxidative stress conditions, the concentrations of H_2O_2 can rise above 100 nM, leading to disruption of normal redox signaling.[3]

H_2O_2 and other ROS are produced by aerobic mitochondrial respiration and metabolism.[2,4,5] Oxidase enzymes such as cholesterol oxidase, nicotinamide adenine dinucleotide phosphate (NADPH) oxidase, glutamate oxidase, lysine oxidase, urate oxidase, oxalate oxidase, lactate oxidase, and glucose oxidase react with their substrate (such as glucose, lactose, etc) to produce H_2O_2.[6,7] Oxidative stress is the results of a high amount of oxidants (ROS) compared to antioxidants in the cellular and extracellular environment. Elevated concentrations of H_2O_2 may also result in accelerated premature ageing, cell injury, damage to biomolecules (such as DNA, proteins and lipids), inhibition of mitochondrial respiration, and apoptosis, which can lead to cancer and many other diseases.[1,8–11,12] Therefore, measurements of H_2O_2 can be used as indicators of health status making it a major intermediate or target in many biosensing strategies.

Many techniques have been developed for the determination and sensing of H_2O_2 for in vivo and ex vivo biological applications.[13,14,15] These techniques include fluorescence,[16,17] chemiluminescence,[18] electron spin resonance[19] and electrochemical methods (Table 1).[17,20]. Fluorescence and chemiluminescence have the potential for low detection limits but they are

susceptible to change in environmental conditions which affect the efficiency of the measurement of H_2O_2. Electrochemical methods have garnered much attention due to their simplicity, low cost, selectivity and sensitivity.[15,21,22]

Table 1. Comparison of some methods of hydrogen peroxide detection

Technique	Advantages	Disadvantages
Fluorescence	Low detection limit	Sophisticated instruments and complex protocol
Chemiluminescence	Low detection limit	Easily be affected by a change in environmental conditions (temperature, the presence of quenchers, pH, etc)
Electron spin resonance	Selective and precise	High cost and sophisticated instruments
Electrochemical methods	Selective, sensitive, stable, and Low cost instruments are used	Electrodes require surface modification

Electrochemical Methods

Electrochemical measurement of H_2O_2 can be achieved through reduction (Equation 1) or oxidation (Equation 2) of H_2O_2 with standard reduction potential (E^0), +1.776 V and oxidation potential, -0.68 V vs. SHE.[23]

$$H_2O_2 + 2H^+ + 2e^- \rightleftharpoons 2H_2O \quad (1)$$

$$H_2O_2 \rightleftharpoons O_2 + 2H^+ + 2e^- \quad (2)$$

Though the E^0 value suggests easy reduction of H_2O_2, in practice, reduction of H_2O_2 typically requires applied potentials on the working electrodes ranging from +0.1 V to -0.6 V vs. SHE reference, while oxidation requires +0.3 to +0.9 V vs. SHE, making them susceptible to interferences from other electrochemical reactions such as oxidation of ascorbic acid and dopamine.[24] Gold and platinum metal electrodes are known as first generation electrodes and

have been used over the years for H_2O_2 detection but their application is hampered by slow electron transfer exhibited by these metal electrodes. Moreover, these metals are costly. To solve this problem of slow electron transfer, organic and inorganic redox mediators were used to facilitate electron transfer between the redox center and the electrode surface. These mediators demonstrated poor selectivity towards H_2O_2 detection. Also, the fabrication of these electrodes was complicated.[25] Ultramicroelectrodes (UMEs) and screen-printed carbon electrodes (SPCEs) are also working electrodes used for H_2O_2 detection. While UMEs exhibit the potential of high selectivity, sensitivity and low detection limit, fabrication of UMEs is a time-consuming process. Recently, screen printed electrodes (SPCEs) have gained much attention due to their ease of fabrication, simplicity, low cost and versatility. However, the application of SPCEs for H_2O_2 detection requires modification of the electrode surface to enhance electron transfer between the electrode surface and the redox center of the analyte. Also, the surface modification of SPCEs enhance the selectivity, sensitivity and detection limit of the electrodes. SPCEs can be treated with metal nanoparticles, carbon nanomaterials, oxygen plasma, nitrogen plasma, Prussian blue, urea, etc to modify the electrode surface.[23]

Surface Modification/Treatment of Electrodes for Hydrogen Peroxide Sensing

In quest for simple and viable means of surface modification of SPCEs to enhance electrode selectivity, sensitivity and give low detection limits, different strategies have been employed over the years. Gonzalez-Sanchez et al.[26] reported a simple way of activating commercially available SPCEs by enhancing the oxidation sites. SPCEs were activated by subjecting them to cyclic voltammetry at 10 mVs^{-1} between 1.0 V and -0.7 V vs. Ag/AgCl in a mixture of 10 mM H_2O_2 and 0.1 M phosphate buffer solution at a pH of 7. While unmodified SPCEs exhibited a sensitivity of 1.7 $\mu A\ mM^{-1}\ cm^{-2}$ for oxidation of H_2O_2 at an applied potential

of 0.7 V vs. Ag/AgCl, a sensitivity of 240 μA mM^{-1} cm^{-2} was achieved for the activated SPCEs under the same conditions.[26]

In another study, Wang et al. found that exposing SPCEs to oxygen plasma using a radiofrequency reactor enhanced the analytical performance of SPCEs towards H_2O_2 reduction. Treated SPCEs exhibited 80-fold sensitivity enhancement for detection compared to untreated SPCEs via amperometry and voltammetry with an applied potential of 0.5 V vs. Ag/AgCl. The enhancement of electrochemical reduction of H_2O_2 on O_2 plasma-treated SPCEs was attributed to the removal of surface contaminants and an increase in the step-like defects on the surfaces of the treated SPCEs in comparison to untreated SPCEs. Poor reproducibility was observed when high powered oxygen plasma was applied.[27]

Prussian blue ($Fe_4[Fe(CN)_6]_3$), its analogues, and nanomaterials have proven over the years to be some of the best materials for surface modification for H_2O_2 reduction with great sensitivity and lowered limit of detection.[28] Prussian blue in its reduced form (Prussian white), potently electrocatalyzes the reduction of H_2O_2 at low potential. Ricci et al. modified SPCEs by drop-casting Prussian blue solution on the working electrode area. This resulted in the enhancement of amperometric detection of H_2O_2 with a sensitivity of 234 μA mM^{-1} cm^{-2} and a lower detection limit of 10^{-7} mol/L. A potential of -0.05 V (vs. internal Ag pseudoreference electrode) was applied in this electrochemical measurement.[29] In separate studies, Du et al. coated multi-walled carbon nanotube with Prussian blue and used electrochemical co-deposition technique to deposit the coated multi-walled carbon nanotube with Prussian blue on a gold electrode. A sensitivity of 856 μA mM^{-1} cm^{-2} and a detection limit of 23 nM was reported with an applied potential of 0.10 V vs. SCE Also, gold electrodes modified multi-walled carbon nanotubes coated with Prussian blue (sensitivity of 428 μA mM^{-1} cm^{-2} and a detection limit of 80

nM) performed better than gold electrodes coated with only Prussian blue.[30] An even lower H_2O_2 detection limit of 10 nM was reported by Zhang et al. by using cubic Prussian blue on single-walled carbon nanotubes and applying a potential of -0.1 V vs. SCE.[31] However, Prussian blue is not stable in alkaline solution because Prussian white is known to dissolve in alkaline solutions. Surface-active agents can be employed to improve the stability of Prussian white electrochemically in alkaline solutions. [32,33]

Platinum nanoparticles and other metal nanomaterials have also proven effective electrode surface modifiers for the detection of H_2O_2. Agrisuelas et al. deposited platinum nanoparticles on SPCEs by recycling used platinum SPEs using aqua regia. A potentiostatic technique was then used to deposit the recovered platinum successfully onto the surface of the screen-printed carbon electrode. This method produced electrodes with a sensitivity of 687.3 μA mM^{-1} cm^{-2} and a detection limit of 1.9 μM by the oxidation of H_2O_2.[34] Chikae et al. deposited Pt nanoparticles onto SPCEs from a solution of $PtCl_2$ by applying a voltage of -0.4 V for 30 s and 200 s.[35] Gold nanoparticles were used by Tangkuaram et al. to modify the surface of screen-printed carbon electrode with the aid of horseradish peroxidase (HRP) in the presence of chitosan and reported that the electrocatalytic activity of the electrode increased after the modification with a limit of detection of 0.65 μM.[36]

Enzymes,[37,38] metal nanoparticles,[39–41] carbon quantum dots,[42,43] carbon nanotubes,[44–46]and carbon-based nanomaterials,[47,48] are also used as electrocatalysts for H_2O_2 reduction. However, many of these methods require time-consuming procedures and/or expensive instrumentation, equipment, or reagents. For these reasons, faster, easier, more economical, and more effective techniques for modifying SPCE has been a subject of great research interest. Nitrogen doping of SPCEs, which involves introducing nitrogen groups onto the electrode

surface, is one modification method that is of particular interest due to its simplicity and success in enhancing the oxygen reduction reaction (ORR) on various carbon materials.[49] Table 2 compares these methods of surface treatment.

Table 2. Comparison of various SPEs surface treatment techniques

Surface treatment technique	Key things to note
Activation of SPCEs with H_2O_2, Oxygen plasma treatment of SPCEs, and	Employs oxidation for H_2O_2 detection. Possible interference (Ascorbic acid, and dopamine)
Platinum and Gold nanomaterials	Platinum and gold are relatively costly.
Use of Prussian blue	Poor stability in alkaline solution
Nitrogen Doping	Simple protocol for nitrogen doping and usually employs reduction of H_2O_2 for detection. Less to no interfering reactions during biosensing.

Nitrogen Doping

Nitrogen doping involves the introduction and incorporation of nitrogen groups such as pyridinic and pyrrolic groups, and quaternary nitrogen groups into the substrate materials as shown in Figure 1. Nitrogen groups are known to be incorporated into the substrate material at the (oxygen-containing sites resulting from the use of carbon black and possible contaminants during the ink formulation) especially carbonyl functional groups on the substrate material.[48,50] For example, during nitrogen doping of graphite using ammonia water as dopant, ammonia as a nucleophile attacks the electrophilic carbon center of the carbonyl functional group to form

amides. At elevated temperatures, the amides undergo cyclization to form nitrogen groups such as pyrrolic and pyridinic nitrogen groups.[51,52]

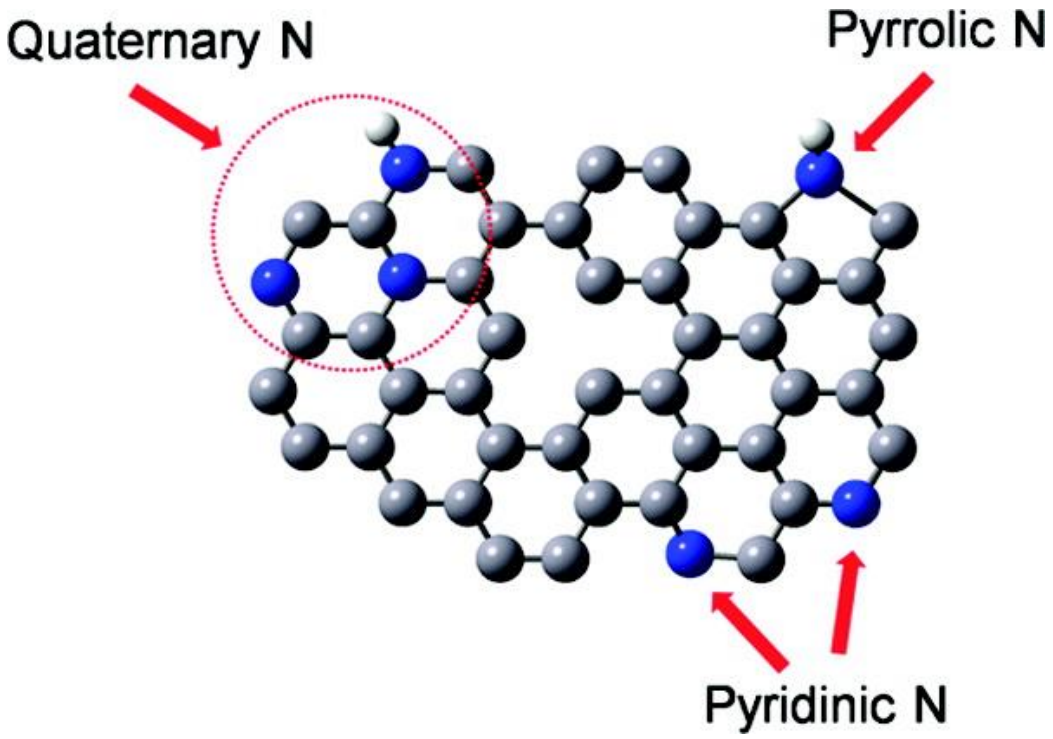

Figure 1.[21] Representation of incorporation of nitrogen groups such as pyridinic and pyrrolic groups and quaternary nitrogen groups into carbon material. Gray balls designate carbon atoms and blue balls represent nitrogen atoms in various nitrogen groups. Reprinted with permission from {Wang, Y.; Shao, Y.; Matson, D. W.; Li, J.; Lin, Y. Nitrogen-Doped Graphene and Its Application in Electrochemilal Biosensing. *J. Nanosci. Nanotechnol.* **2010**, *4* (4), 1790–1798 ▪. https://doi.org/10.1021/nn100315s}. Copyright {2010}. American Chemical Society.

Nitrogen doping can be achieved through various methods, such as nitrogen plasma treatment of graphene,[53] pyrolysis of iron(II)phthalocyanine,[49] hydrothermal treatment of carbon nanofiber powder with urea[54] and heating graphene nanoribbon in the presence of ammonium hydroxide.[48] Nitrogen doping of carbon materials introduce free electrons at the active sites, which facilitate O-O bond breakage in H_2O_2 reduction. Shi et al. doped graphene nanoribbons

with ammonia water and drop cast the N-doped graphene nanoribbons on fabricated SPCEs. The doping of graphene nanoribbons was achieved by mixing synthesized graphene nanoribbons and aqueous ammonia and heating it. This method successfully introduced 4.3% pyridinic and pyrrolic nitrogen groups onto the nitrogen-doped SPCEs based on X-ray photoelectron spectroscopy (XPS). The primary site for the incorporation of nitrogen-containing species during the nitrogen doping process is the oxygen functionality sites. They reported that the modified electrodes exhibited enhanced electrocatalytic activity towards H_2O_2 reduction with an amperometric response range from 5 to 2785 uM H_2O_2 and a limit of detection of 1.7 uM at an applied potential of -0.4 V vs. Ag/AgCl.[48]

Wu et al.[55] used density functional theory (DFT) calculations and simulations to gain insight into the effect nitrogen doping has on H_2O_2 reduction on graphene-based carbon materials. The group observed stronger (more stabilized) adsorption of H_2O_2 on N-doped graphene (physisorption) compared to pristine graphene. Electrostatic potential (EP) calculations suggest fewer reactive sites (sites for adsorption/O-O bond breakage) on pristine graphene (limited to edges) compared to N-doped graphene, which exhibits a positive electrostatic potential region near doped N atom, providing a reactive site for H_2O_2 adsorption and reduction The order of reactivity was then determined to be pyridinic N-doped graphene > pyrrolic N-doped graphene > graphitic N- doped graphene > pristine graphene. H_2O_2 reduction proceeds after adsorption, the O-O bond could be broken by accepting an H^+ to form water and leave the surface. A chemical bond formation between C-O is followed. Another way by which O-O bond is broken is by a spontaneous disintegration of the O-O bond and forming two OH groups on the carbon surface (unfavorable).[55]

Liu et al. recently introduced a method known as soft nitriding to modify carbon black and other carbon materials with surface nitrogen. This is a metal-free strategy that involves low-temperature annealing of carbon supports with urea. The thermal decomposition of urea produces ammonia and isocyanic acid which react with the oxygen-containing sites on the carbon supports. These sites can serve as a primary location where nitrogen functional groups are incorporated. They reported the presence of 17% quaternary nitrogen groups, 68% amine and amide nitrogen groups and 15% pyridinic groups on the carbon supports after the doping process based on XPS. The presence of these groups made the nitrogen-doped carbon supports a viable precursor for subsequent work involving the deposition of ultrasmall, electrocatalytic metal nanoparticles.[56]

Liu's method of nitrogen doping was employed by Ogbu et al. to fabricate nitrogen-doped SPCEs (N-SPCEs) from laboratory-formulated inks based on graphite powder. Interestingly, though graphite lacks oxygen functional groups that typically serve as sites for incorporation of nitrogen groups during doping, XPS results showed that thermal decomposition of urea in the presence of graphite did introduce nitrogen functional groups on the carbon support. Surface analysis revealed the nitrogen atoms to originate from the presence of 1,3,5-triazines, which originate from well-documented condensation and polymerization reactions that occur upon further thermal treatment of urea and isocyanic acid. 1,3,5-triazines can strongly adsorb to graphite, adsorb between graphene layers, and interact through hydrogen bonding. A sensitivity of 264 μA mM^{-1} cm^{-2} and detection limit of 2.5 μM was reported for H_2O_2 reduction on N-SPCEs. While these studies proved that soft nitriding can be used to prepare N-SPCEs for H_2O_2 reduction, further enhancement may be possible through the selection of a carbon material that contains surface oxygen to facilitate soft nitriding as reported by Liu et al.[57]

Research Aims

The studies by Ogbu proved that nitrogen doping of graphite and formulating ink from it is a viable route to prepare N-SPCEs for H_2O_2 detection. While this is true, the preparation of laboratory formulated graphite ink for N-SPCEs fabrication is time-consuming. Hence, commercially available graphite ink was used in this study (based on previous work in our laboratory by Ogbu et al. for easy comparison of results) to simplify the procedure for the fabrication of N-SPCEs. Also, Shi's method[48] of nitrogen doping with ammonia water introduced 4.3% nitrogen groups onto the electrode surface and yet the electrodes exhibited enhanced electrochemical performance and a sensitivity of 2180 $\mu A\ mM^{-1}\ cm^{-2}$ which is 8 times higher compared to sensitivity reported by Ogbu in the previous study.[58] This result influenced the use of Shi's method and ammonia water as a dopant to introduce nitrogen groups onto SPCEs in this study.

The goal of this study is to produce N-SPCEs with lower detection limits and high sensitivity which could be used for biosensing. To achieve this, SPCEs would be fabricated from commercially available graphite ink and Shi's method of nitrogen doping would be used to prepare N-SPCEs from already printed SPCEs. SPCEs and N-SPCEs would be characterized by XPS and electrochemical techniques. Also, the performance of SPCEs would be compared to N-SPCEs as the amperometric response of both N-SPCEs and SPCEs towards H_2O_2 reduction would be investigated.

CHAPTER 2. EXPERIMENTAL

Materials

The chemicals were all purchased and used as received from the manufacturer. Ammonium hydroxide (28-30%) was obtained from VWR Analytical. Ferrocenemethanol, potassium ferricyanide, potassium ferrocyanide, potassium chloride, and bovine calf serum were received from Sigma Aldrich. Carbon graphite paste and dielectric paste were purchased from the Gwent group. Ultra-high purity nitrogen was obtained from Airgas Mid-America. Hydrogen peroxide (30 wt%) and phosphate buffer saline (PBS) were purchased from Fisher Scientific. A Millipore Synergy purification system was used to produce 18.2 MΩ·cm ultrapure water from deionized water. All the aqueous solutions were prepared using ultrapure water.

Instruments

PHI VersaProbe III scanning XPS microscope and monochromatic Al K-alpha X-ray source (Dr Xu Feng at Virginia Tech carried out XPS characterization) and CH Instruments 760E electrochemical workstation.

SPCE Fabrication and Nitrogen Doping

SPCEs were manually fabricated from commercially available carbon graphite paste deposited on plastic cellulose acetate sheets (cut into 2 cm x 4 cm rectangular shape) with the aid of a 110-mesh screen as previously reported (Figure 2).[59] The screen was firmly placed on the plastic cellulose acetate sheets as the ink was placed and pressed through the mesh. The ink was then deposited on the rectangular plastic cellulose acetate sheet. The procedure was repeated for other electrodes. The electrodes were cured for 30 minutes in an oven at a temperature of 60 $^{\circ}$C and kept at room temperature until ready for use. Nitrogen doping of SPCEs was carried out

by submerging the SPCEs in 200 mL 0.6 M ammonia water and heating the content to 80 °C while the system was left open throughout the doping period.[48] After one to six hours, the electrodes were rinsed with deionized water, air-dried at room temperature for an hour and dielectric paste was printed over the conductive path connecting the working electrode and contact pad portions of the SPCEs. Geometric areas of the working electrodes of bare and nitrogen doped SPCEs were obtained using photographic images that were processed using ImageJ software.

Figure 2. Sample electrodes fabricated from commercially available graphite ink and nitrogen-doped. The lower circular end of the electrodes denotes the working portion of the electrodes while connections to electrochemical systems are done at the other end.

Electrochemical Measurements and Electrode Characterization

SPCEs were characterized by voltammetry and amperometry. All electrochemical measurements were carried out using a CH Instruments 760E electrochemical workstation. Platinum wire was used as a counter electrode, Ag/AgCl (1 M KCl filling solution) as the

reference electrode and fabricated SPCE or N-SPCE as the working electrode. Currents from electrochemical measurements were converted to current densities by dividing by the geometric areas of the individual working electrodes.

Cyclic Voltammetry

A solution of 0.5 mM ferrocenemethanol was prepared in 0.1 M potassium chloride. Approximately, 15 mL of the solution was placed in a beaker and was used to characterize the fabricated bare and modified electrodes (SPCEs and N-SPCEs). Using the fabricated electrodes as the working electrode, the reference and the counter electrodes were suitably inserted into the 15 mL solution (with the circular end of the working electrode in contact with the solution). At a scan rate of 50 mV/s, cyclic voltammetric measurements of the fabricated bare and modified electrodes were taken and the peak separation on each electrode was determined.

Further studies of these electrodes were conducted in 0.01 M phosphate buffer saline solution. Here, about 15 mL of phosphate buffer saline was taken into a beaker and cyclic voltammetric measurements of the various electrodes were conducted. Also, 15 mL of the phosphate buffer solution was degassed with ultrapure nitrogen gas and cyclic voltammetry of the various electrodes were taken.

Furthermore, a 20 mM solution of H_2O_2 in 0.01 M phosphate buffer solution was prepared. About 15 mL two portions of the solution were taken with one degassed using ultrapure nitrogen gas and cyclic voltammetry of the various electrodes were obtained. All the CVs were taken at a scan rate of 50 mV/s.

Amperometric Measurements

Approximately 30 mL of 0.01 M phosphate buffer saline (PBS) solution was poured into a beaker. The solution was degassed with ultrapure nitrogen gas for 10 minutes. While stirring

with a magnetic stirrer, the electrodes (working, reference and counter) were placed in the beaker and an amperometric background measurement of the electrode was taken until the electrodes became stable. After this, amperometric measurements were taken by injecting three times each with a micropipette 20 µL, 40 µL, 60 µL, 150 µL (10 mM H_2O_2), 30 µL, 60 µL, 90 µL, 150 µL, 300 µL, 360 µL, 450 µL and 600 µL (100 mM H_2O_2) into the 30 mL 0.01 M phosphate buffer solution to produce concentrations of 0.02 mM, 0.06 mM, 0.119 mM, 0.263 mM, 0.553 mM, 1.129 mM, 1.981 mM, 3.368 mM, 6.028 mM, 9.032 mM, 12.523 mM, 16.791 mM. The process was repeated for each fabricated bare and modified electrode. The injections were done sequentially for each electrode measurement. Calibration curves were plotted from the results and sensitivities determined.

X-Ray Photoelectron Spectroscopy (XPS)

Dr Xu Feng at Virginia Tech carried out XPS characterization of one of each SPCEs and 6 hours doped N-SPCEs using PHI VersaProbe III scanning XPS microscope and monochromatic Al K-alpha X-ray source (1486.6 eV). XPS spectra were acquired with 200 µm/50 W/15 kV X-ray settings and dual beam charge neutralization. All binding energies were referenced to sp^2 carbon peak at 284.3 eV. Atomic concentration % of elements were determined from the integrated intensity of the elemental photoemission features corrected by relative atomic sensitivity factors.

CHAPTER 3. RESULTS AND DISCUSSION

Electrochemical Characterization of SPCEs and N-SPCEs

SPCEs were successfully fabricated and cured. They were 2.8 cm long and the geometric average surface area of the of SPCEs (four electrodes) and N-SPCEs (four electrodes) were determined to be 0.040 (±0.005) cm^2 and 0.034 (±0.004) cm^2, respectively. The electrodes were then doped with ammonia water and when they were ready, electrochemical characterization were carried out.

Cyclic voltammetry (CV) was used to characterize the bare and modified screen-printed carbon electrodes. Ferrocenemethanol (0.5 mM ferrocenemethanol was prepared in 0.1 M potassium chloride), a well-known redox probe that undergoes reversible one-electron oxidation was employed in this process. CV sweeps of SPCE and N-SPCE (doped for 4 hours) working electrodes between potentials of -0.4 V and +0.4 V (vs. Ag/AgCl). The voltammetric average peak to peak separation for the SPCEs and N-SPCEs was found to be 119.5 ± 14 mV and 90.8 ± 5 mV respectively (Figure 3) based on three electrodes each. For an ideal reversible one-electron transfer redox probe like ferrocenemethanol, the voltammetry peak to peak separation is expected to be 59 mV but in reality, the peak separations are usually large.[60] These peak separations are comparable to commercially available screen-printed carbon electrodes.[58,61,62]

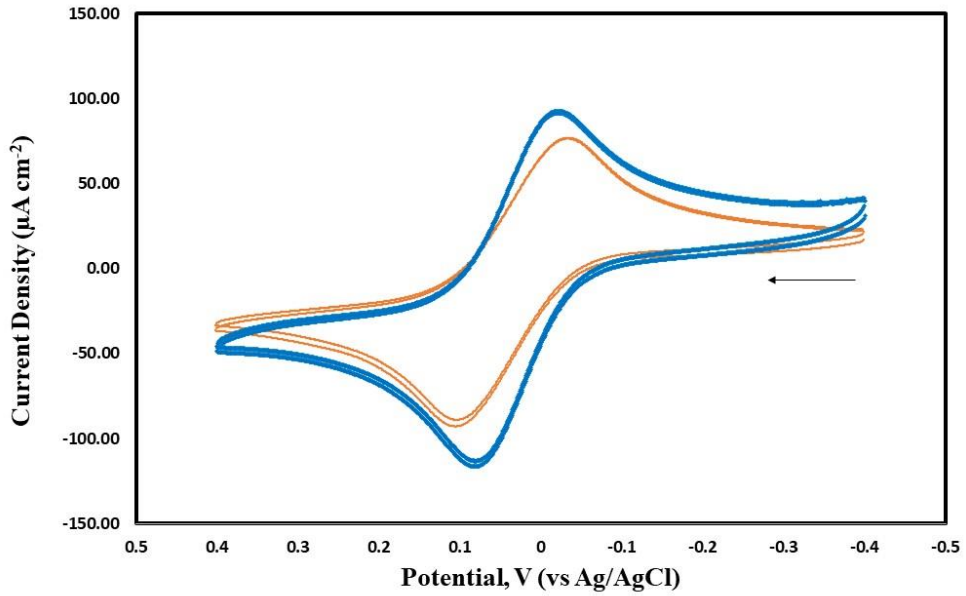

Figure 3. Representative CVs of SPCE (orange) and N-SPCE (blue) in 0.5 mM ferrocenemethanol with 0.1 M potassium chloride. The arrow indicates the direction of the scan. CV. The scan rate was 50 mV s^{-1}.

Electrocatalytic Activity of Modified Screen-Printed Carbon Electrodes

To investigate the response of SPCEs and N-SPCEs (doped for 4 hours) towards H_2O_2, CVs were taken in the presence and absence of H_2O_2 in 0.01 M PBS (Figure 7). N-SPCEs showed electrocatalytic activity towards the reduction of H_2O_2 after it was exposed to 20 mM H_2O_2 (Figure 4B) with 60-folds current enhancement compared SPCEs. Undoped electrodes (Figure 4A) showed a small change in current density upon exposure to 20 mM H_2O_2 with an onset potential of 0.39 V. From the voltammogram, N-SPCEs exhibited a positive shift in the onset potential, which was determined to be approximately 0.16 V. This is comparable with previous work.[58] The results obtained here indicate that nitrogen doping with ammonia water

worked with screen-printed graphite electrodes and could be used as an electrocatalyst for hydrogen peroxide reduction. The results are comparable with the literature.[21,48,54]

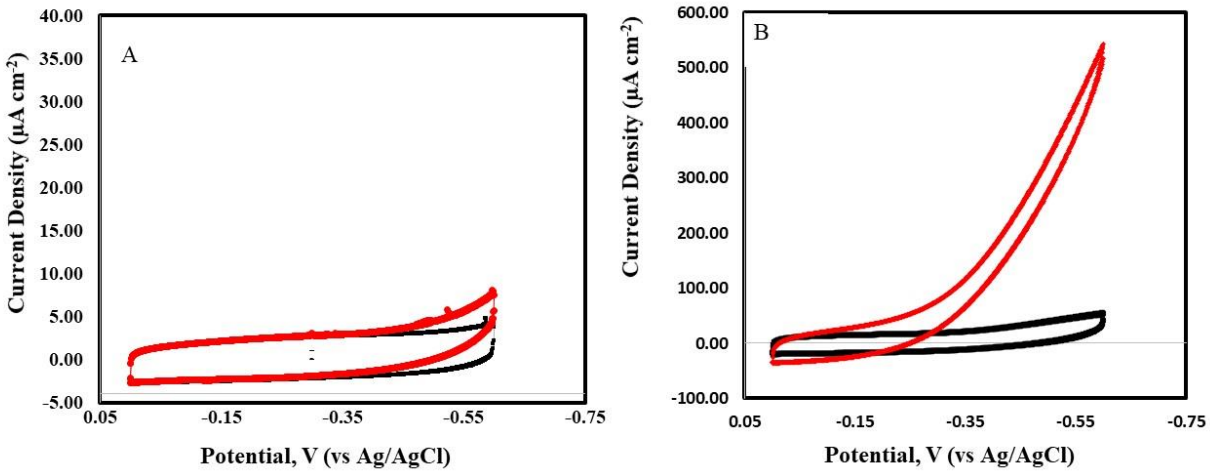

Figure 4. CVs in 0.01 M PBS at a scan rate of 50 mVs^{-1} representing the response in the absence (black) and presence (red) of 20 mM hydrogen peroxide. A) SPCE. B) N-SPCE (doped for 4 hours) .

Amperometric Detection of Hydrogen Peroxide Using Modified Electrodes

Amperometric responses of SPCEs and N-SPCEs (doped for 4 hours) towards H_2O_2 reduction were taken by successively injecting different volumes of 10 mM H_2O_2 and 100 mM H_2O_2 three times with each volume (20 µL, 40 µL, 60 µL, 150 µL and 30 µL, 60 µL, 90 µL, 150 µL, 300 µL, 360 µL, 450 µL, 600 µL respectively) into the 30 mL stirred 0.01 M PBS solution at a pH of 7.4 (Figure 5) while applying a potential of -0.4 V (vs. Ag/AgCl) to the SPCE or N-SPCE working electrode. SPCEs demonstrated showed small change in current density upon the injection of varying concentrations of H_2O_2. On the other hand, N-SPCEs showed a rapid and significant stepwise increase in current density upon the injection of varying concentrations of

H_2O_2 into the 0.01 PBS solution. A good linear relationship ($R^2 = 0.9697$) was shown between the concentration of hydrogen peroxide and current density with good reproducibility. At higher concentrations, the calibration curve begins to deviate from linearity, and this resulted in two linear ranges with 0.02 to 0.553 mM and 1.129 mM to 16.791 mM with the lower concentration linear range being the most useful. The average sensitivities of two N-SPCEs were determined from two linear ranges 0.02 to 0.553 mM and 1.129 mM to 16.791 mM to be 18.19 $\mu A\ mM^{-1}\ cm^{-2}$ and 9.00 $\mu A\ mM^{-1}\ cm^{-2}$ the slopes of the calibration curves. At higher concentrations, the curve begins to deviate from linearity. The detection limit was then calculated by multiplying 3 by the standard deviation of the background and dividing by the sensitivity to be 3.53 µM. The sensitivity obtained here is 11 times lower compared to previous work from our laboratory.[58] The difference may have resulted from the doping strategies employed in each case (they doped graphite first and made N-SPCEs but here, the electrodes were prepared before doping was done). Though the sensitivities of the SPCEs and the N-SPCEs are comparable with other work.[26]

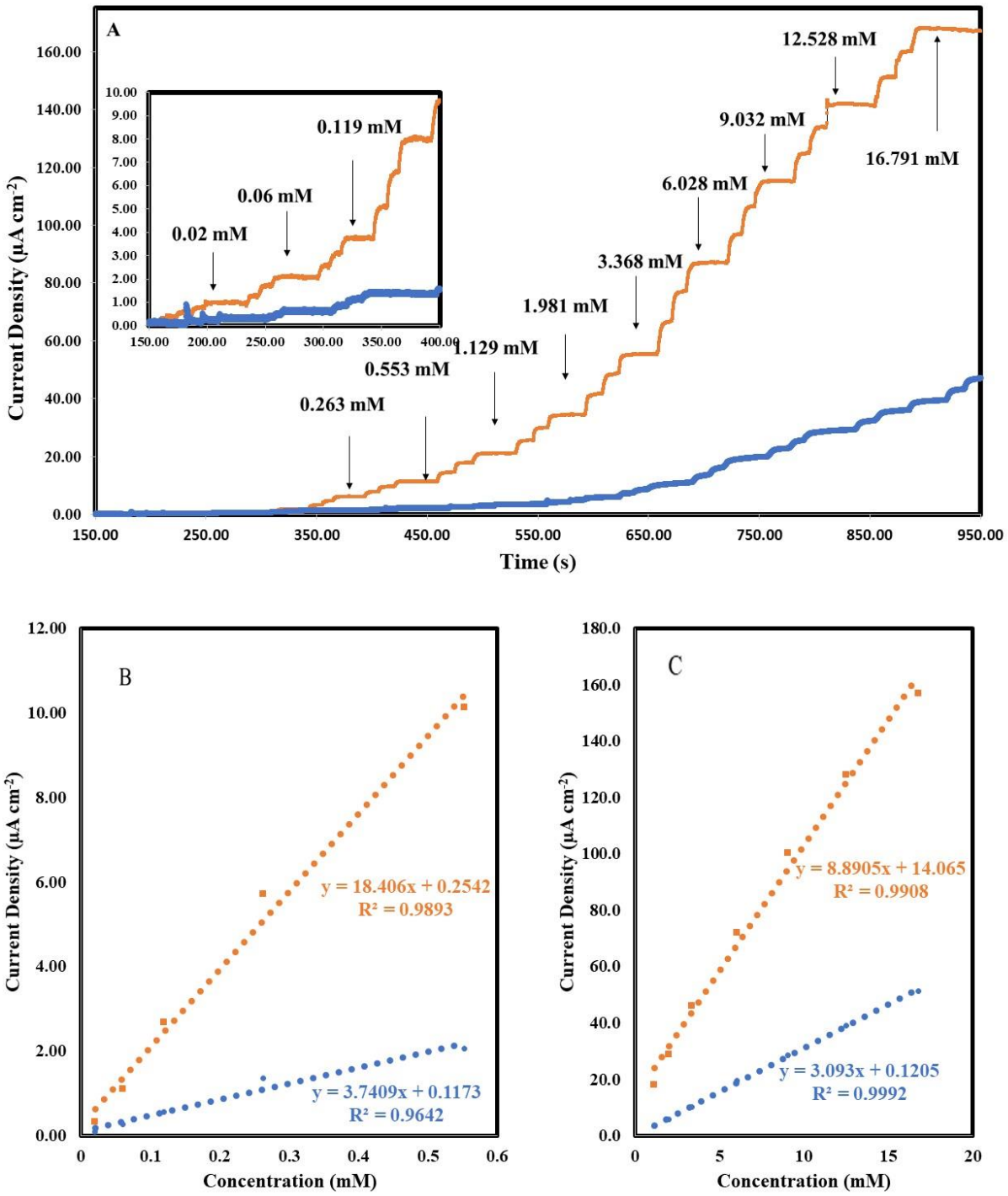

Figure 5. A). Representative amperometric response of SPCEs (blue) and N-SPCEs (orange) towards H_2O_2 detection. The arrows in A) indicate various concentrations resulting from the successive injections of H_2O_2. Calibration curves of N-SPCE (orange) and SPCE (blue) for the detection of H_2O_2 through amperometry for the two linear ranges, B). Concentration ranges from 0.02 to 0.553 mM and C). Concentration ranges from 1.129 mM to 16.791 mM.

Optimization of Nitrogen-Doped Screen-Printed Carbon Electrodes

Optimization experiments were conducted based on the duration of the doping process to further enhance the sensitivity of the electrodes. The electrodes were doped with ammonia water at a temperature of 80 °C for 1, 2, 4 and 6 hours. Various calibration curves (Figures 6A to 6D) were plotted to obtain the sensitivity of the electrodes

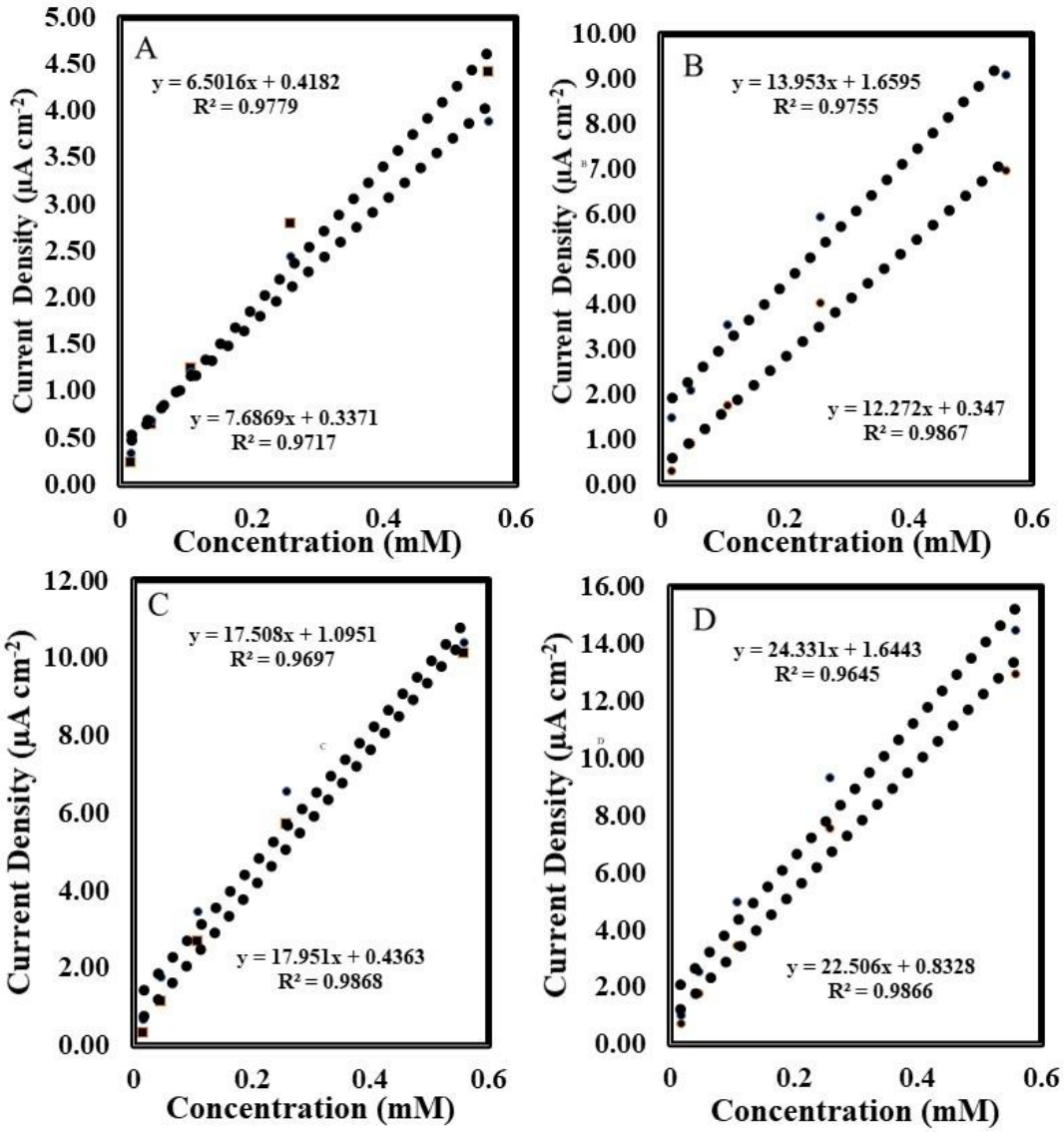

Figure 6. Calibration curves of two N-SPCEs each at different doping durations. (A). 1 hour doping. (B). 2 hours of doping. (C). 4 hours doping. (D). 6 hours of doping

Varying the doping period of the electrodes revealed a good relationship between the doping time and the sensitivity of the electrodes. As the doping period increased, the sensitivity of the electrodes was enhanced (Figure 7). This may be because more nitrogen groups can be incorporated into the carbon material at a prolonged duration.

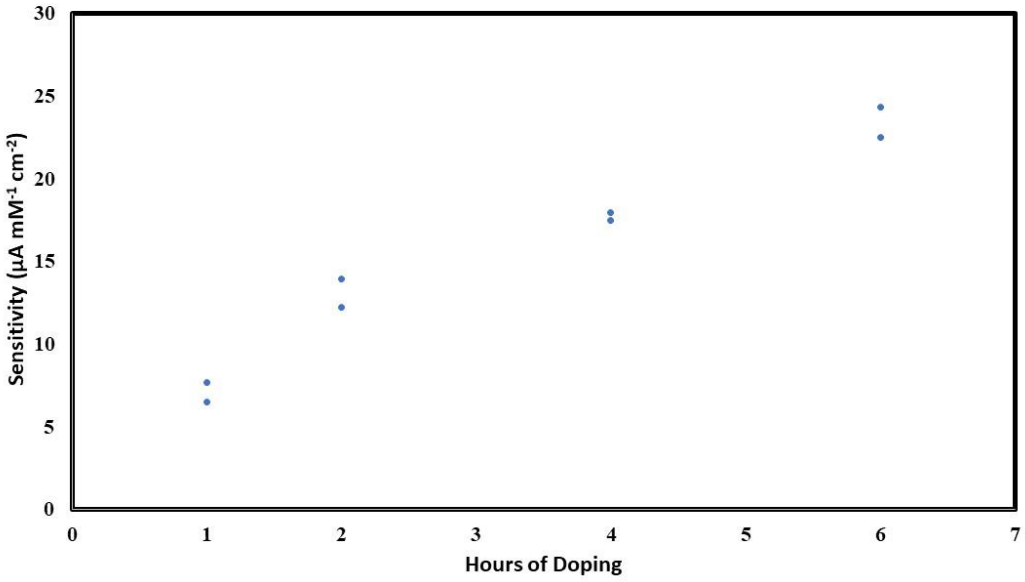

Figure 7. A schematic representation of the relationship between the hours of doping and the sensitivity of the electrodes. Duplicate experiments using two different electrodes that were doped for the same amount of time are presented for each doping time.

Comparing the sensitivity obtained here to the sensitivities of electrochemically activated commercial screen-printed platinum (SPPtEs) and Prussian blue (PB-SPCEs) electrodes determined to be 40 µA mM^{-1} cm^{-2} and 26 µA mM^{-1} cm^{-2} respectively, 24.33 µA mM^{-1} cm^{-2} obtained in this study (after 6 hours of doping) is comparable with these commercial SPEs. SPCEs used in this work exhibited quite a higher sensitivity (3.74 µA mM^{-1} cm^{-2}) compared to commercially available SPCE (1.71 µA mM^{-1} cm^{-2}) reported in previous work (Table 3).[26] Ledru et al. reported that the quantity of polymeric binder used in making these inks for SPCEs has a

great effect on the sensitivity of the electrodes. An increase in polymeric binder ratio decreases the sensitivity of the electrode by minimizing the diffusion rate of H_2O_2. The polymeric binder used in the graphite ink might have influenced the lower sensitivity observed here.[38]

Table 3. Comparison of electrochemical performance of some screen-printed electrodes for hydrogen peroxide sensing

Electrode	**E(V)[a]**	**Linear Range (mM)**	**Sensitivity** ($\mu A\ mM^{-1}\ cm^{-2}$)	**Limit of Detection** (μM)	**Ref.**
N-SPCE	-0.4	0.02-5.3	264	2.5	[58]
N-GrNRs/SPCE	-0.4	0.005-0.085 0.135-1.285	154.78, 45.44	1.72	[48]
Pd-CNT/SPCE	-0.3	0.1-1.0	NR[d]	20	[65]
AuNPs-SPCE	-0.35	0.003-0.243	NR[d]	0.6	[66]
PPy-HRP/SPCE	-0.3	0.1-2.0	33.24	-	[67]
CuSPCE	-0.3	0-0.2	NR[d]	0.97	[68]
PtNP/rGO–CNT/PtNP/SPCE	-0.28	0.025-1	206	4.3	[69]
HRP-SPCEs	0[c]	0.01-0.25	37[b]	NR[d]	[38]
O_2-Plasma-SPCEs	+0.5[c]	NR[d]	5.2[b]	NR[d]	[27]
H_2O_2-activated-SPCEs	+0.7[c]	NR[d]	240[b]	NR[d]	[26]
SPPtEs	+0.7[c]	NR[d]	40[b]	NR[d]	[26]
PB-SPCEs	-0.1	NR[d]	26[b]	NR[d]	[26]
N-SPCE	-0.4	0.02-0.553 1.129-16.791	24.33 7.63	2.64	This work

[a] working electrode potential vs. Ag/AgCl reference, [b] based on geometric area of the working electrode, [c] based on oxidation of H_2O_2, [d] not reported.

Nitrogen-Doped Screen-Printed Carbon Electrode (N-SPCEs)

Survey XPS surface analysis of the SPCEs and N-SPCEs were conducted, and they demonstrated a significant difference between SPCEs, and 6 hours doped N-SPCEs (Figure 8). Elemental constituents of the surface of SPCEs were determined to be 93.3%, 6.42%, and 0.28% for C, O, and N respectively (Table 4). The C1s, O1s and N1s peaks for both SPCEs and N-SPCEs were observed at 284.3 eV, 531.9 eV and 399.9 eV respectively (Figure 8) and are comparable to previous work.[48,63] Cl2s and Cl2p peaks were present on both SPCEs and N-SPCEs as shown in figure 3. Poly(vinyl chloride), poly(vinyl alcohol) and poly(vinyl acetate) are polymeric binders used in ink preparation. Among these binders, Poly(vinyl chloride) is the most used. The presence of these Cl2s and Cl2p peaks suggest poly(vinyl chloride) was used polymeric binder in the ink formulation.[64] Comparing the percent atomic concentration of nitrogen in N-SPCEs to SPCEs, the nitrogen doping technique elevated the percent atomic concentration of nitrogen by 1.06%. This means that nitrogen doping with ammonium water worked on graphite electrodes though percent nitrogen atoms are 31 times lower compared to 32.9% previously reported by Ogbu. Shi et al. reported 4.3% nitrogen atoms on their nitrogen-doped graphene nanoribbons which were achieved by thermal treatment of the nanoribbons with ammonium hydroxide.[48] A higher percentage of nitrogen 32.9% for their N-SPCEs was reported by Ogbu et al. after doping graphite with urea.[58] 1.34 % of nitrogen atom concentration here may have resulted from the differences in doping material, doping strategy, and/ carbon material.

Table 4. Relative atomic % composition of C, N, and O for SPCEs and N-SPCEs

Electrode	Carbon	Oxygen	Nitrogen
SPCEs	93.30	6.42	0.28
N-SPCEs	90.62	8.02	1.34

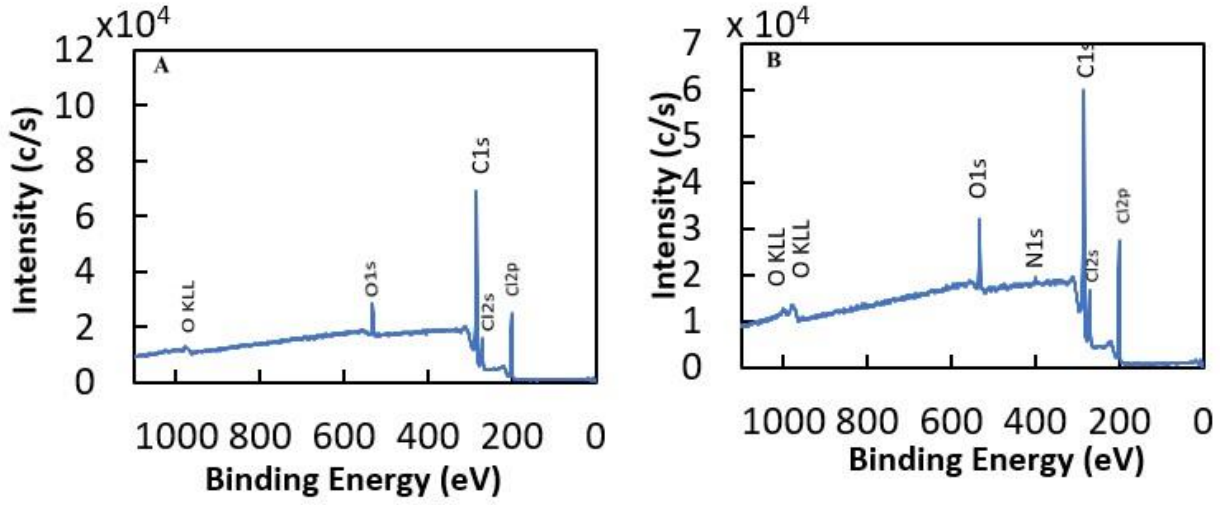

Figure 8. XPS spectra for A). SPCEs and B). N-SPCEs

Shi et al. reported that nitrogen doping with ammonia water reduced some oxidized species on pristine graphene.[48] On the contrary, our spectra suggest that nitrogen doping with ammonia water increased the oxygen-containing sites on the graphite electrode. Figure 9 revealed that sp^2 and sp^3 peaks at 284.26 eV and 285.00 eV on the deconvoluted C 1s peaks for SPCEs reduced compared to C1s peaks of N-SPCEs. Deconvoluted spectrum for N-SPCEs showed an increase in atomic concentration of C-O and C=O groups. The increase in % atomic concentration C=O can also be attributed to the presence of C-N bonds because the peaks associated with C-N and C=O are known to overlap with binding energies of approximately 287 to 288 eV.[63] This makes it difficult to confirm the presence of C-N peaks on the C1s peaks at approximately 288 eV.

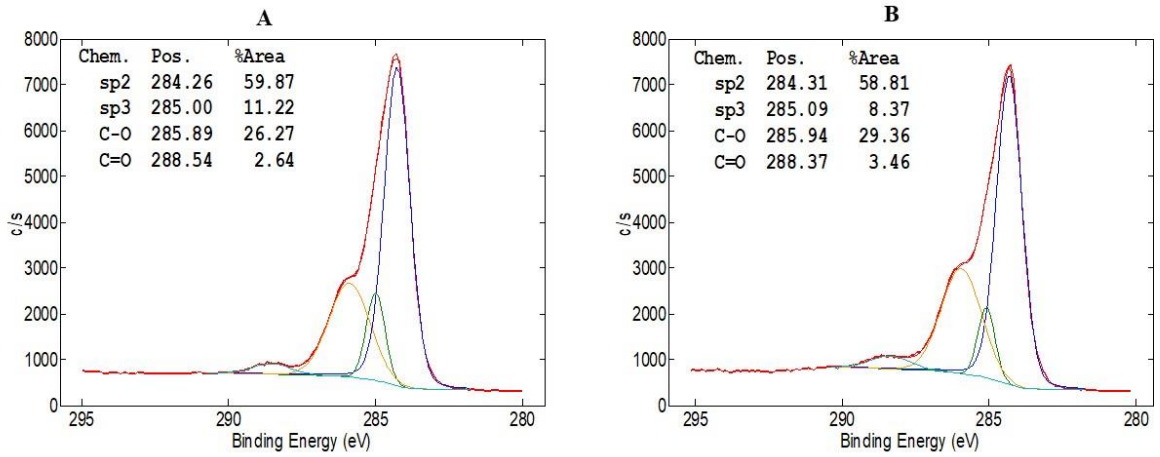

Figure 9. Deconvoluted XPS spectra of C1s A). SPCEs and B). N-SPCEs (Raw data – red curve, sp^2 284 eV – blue curve, sp^3 285 – green curve, C-O 285.9 eV – yellow curve and C=O 288 eV – light blue curve)

Deconvoluted N1s peak showed two peaks on N-SPCEs positioned at 399,88 eV and 399.92 eV respectively. Shi et al. attributed the N1s peaks at 399.7 eV and 400.6 eV to pyridinic and pyrrolic nitrogen groups respectively.[48] These values are comparable to the N1s peaks (Figure 10) here which suggest the ammonia water doping elevated the content of pyridinic and pyrrolic groups on the graphite electrodes.

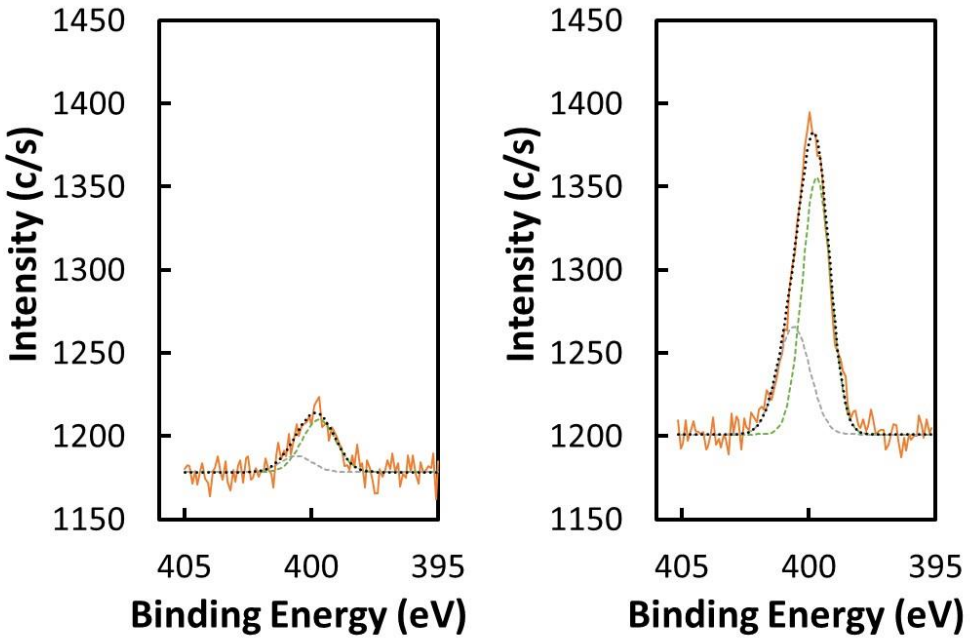

Figure 10. Deconvoluted N1s peaks A). SPCEs and B).N-SPCEs (Raw data – orange curve, black dotted line- modeled curve, pyrrolic curve - gray and pyridinic curve – green curve)

CHAPTER 4. CONCLUSION AND FUTURE WORK

Conclusion

SPCEs were fabricated using low cost commercially available graphite ink. The average electrode size was determined to be 0.040 (±0.005) cm^2 and 0.034 (±0.004) cm^2 for SPCEs and N-SPCEs respectively. Ammonium hydroxide was used to modify the SPCEs to produce N-SPCEs. XPS results indicated the presence of pyridinic nitrogen groups on the electrode surface.

The electrochemical performance of the electrodes was evaluated using cyclic voltammetry and amperometry. Cyclic voltammograms of SPCEs and N-SPCEs in 0.01 PBS solution at a pH of 7.4 in the presence of 20 mM H_2O_2 showed an about 60-fold increase in current density for N-SPCEs with an onset potential of -0.18 V compared to SPCEs with an onset potential of -0.38 V. The amperometric response of SPCEs and N-SPCEs was also determined by applying a potential of -0.4 V in PBS and the sensitivities were found to be 3.74 $\mu A\ mM^{-1}\ cm^{-2}$ and 24.33 $\mu A\ mM^{-1}\ cm^{-2}$ respectively. The sensitivity of N-SPCEs is 6 times that of SPCEs. The sensitivity of N-SPCEs were determined to be 2.64 µM.

N-SPCEs showed enhanced electrocatalytic activity towards H_2O_2 reduction by the responses from CV and amperometry. This can be attributed to the presence of nitrogen groups on the electrode surface which facilitate electron transfer kinetics and the adsorption of H_2O_2 and subsequent breakage of O-O bonds in the presence of H^+ ions.

Optimization of the electrode sensitivity by varying the doping period showed significant enhancement of the sensitivity of the electrode from 6.5 $\mu A\ mM^{-1}\ cm^{-2}$ to 24.33 $\mu A\ mM^{-1}\ cm^{-2}$ for 1 to 6 hours of doping.

Future Work

Though the sensitivities of the electrodes are low compared to previous work, the method of fabrication and doping is simple and precise. Hence, we will increase the doping time and vary the concentration of dopant, this may introduce more nitrogen groups on the electrode and enhance the electrode sensitivity and selectivity.

Also, it is reported that during the nitrogen doping process, the nitrogen groups react with the oxygen sites on the surface of the electrode and that is how the nitrogen groups are incorporated onto the electrode surface.[56] Because increasing the oxygen-containing sites may enhance the incorporation of nitrogen-containing groups on the electrode which has the potential of increasing the sensitivity of the electrode. We will be subjecting SPCEs to cyclic voltammetry at 10 mVs^{-1} between +1.0 V and -0.7 V (vs. Ag/AgCl) in a mixture of 10 mM hydrogen peroxide and 0.1 M phosphate buffer solution at a pH of 7. This method is known to introduce more oxygen-containing sites on the SPCEs. Hence, doping SPCEs after subjecting them to this method may be a great way of optimizing the sensitivity and selectivity of the electrodes.

REFERENCES

(1) Halliwell, B.; Clement, M. V.; Long, L. H. Hydrogen Peroxide in the Human Body. *FEBS Lett.* **2000**, *486* (1), 10–13.

(2) Caruso, A. A.; Del Prete, A.; Lazzarino, A. I. Hydrogen Peroxide and Viral Infections: A Literature Review with Research Hypothesis Definition in Relation to the Current Covid-19 Pandemic. *Med. Hypotheses* **2020**, *144* (April), 109910. https://doi.org/10.1016/j.mehy.2020.109910.

(3) Sies, H. Hydrogen Peroxide as a Central Redox Signaling Molecule in Physiological Oxidative Stress: Oxidative Eustress. *Redox Biol.* **2017**, *11* (November 2016), 613–619. https://doi.org/10.1016/j.redox.2016.12.035.

(4) Sies, H. Role of Metabolic H2O2 Generation: Redox Signaling and Oxidative Stress. *J. Biol. Chem.* **2014**, *289* (13), 8735–8741. https://doi.org/10.1074/jbc.R113.544635.

(5) Jones, D. P.; Sies, H. The Redox Code. *Antioxidants Redox Signal.* **2015**, *23* (9), 734–746. https://doi.org/10.1089/ars.2015.6247.

(6) Chen, W.; Cai, S.; Ren, Q. Q.; Wen, W.; Zhao, Y. Di. Recent Advances in Electrochemical Sensing for Hydrogen Peroxide: A Review. *Analyst* **2012**, *137* (1), 49–58. https://doi.org/10.1039/c1an15738h.

(7) Pollack, B.; Holmberg, S.; George, D.; Tran, I.; Madou, M.; Ghazinejad, M. Nitrogen-Rich Polyacrylonitrile-Based Graphitic Carbons for Hydrogen Peroxide Sensing. *Sensors (Switzerland)* **2017**, *17* (10), 1–12. https://doi.org/10.3390/s17102407.

(8) Sosa, V.; Moliné, T.; Somoza, R.; Paciucci, R.; Kondoh, H.; LLeonart, M. E. Oxidative Stress and Cancer: An Overview. *Ageing Res. Rev.* **2013**, *12* (1), 376–390. https://doi.org/10.1016/j.arr.2012.10.004.

(9) Szypowska, A. A.; Burgering, B. M. T. The Peroxide Dilemma: Opposing and Mediating Insulin Action. *Antioxidants Redox Signal.* **2011**, *15* (1), 219–232. https://doi.org/10.1089/ars.2010.3794.

(10) Tocchetti, C. G.; Stanley, B. A.; Murray, C. I.; Sivakumaran, V.; Donzelli, S.; Mancardi, D.; Pagliaro, P.; Gao, W. D.; Van Eyk, J.; Kass, D. A.; Wink, D. A.; Paolocci, N. Playing with Cardiac Redox Switches: The HNO Way to Modulate Cardiac Function. *Antioxidants Redox Signal.* **2011**, *14* (9), 1687–1698. https://doi.org/10.1089/ars.2010.3859.

(11) Oliver, C. N.; Ahn, B. W.; Moerman, E. J.; Goldstein, S.; Stadtman, E. R. Age-Related Changes in Oxidized Proteins. *J. Biol. Chem.* **1987**, *262* (12), 5488–5491.

(12) Chen, Q.; Vazquez, E. J.; Moghaddas, S.; Hoppel, C. L.; Lesnefsky, E. J. Production of Reactive Oxygen Species by Mitochondria: Central Role of Complex III. *J. Biol. Chem.* **2003**, *278* (38), 36027–36031. https://doi.org/10.1074/jbc.M304854200.

(13) Charisiadis, P.; Tsiafoulis, C. G.; Exarchou, V.; Tzakos, A. G.; Gerothanassis, I. P. Rapid and Direct Low Micromolar NMR Method for the Simultaneous Detection of Hydrogen Peroxide and Phenolics in Plant Extracts. *J. Agric. Food Chem.* **2012**, *60* (18), 4508–4513. https://doi.org/10.1021/jf205003e.

(14) Tanaka, A.; Iijima, M.; Kikuchi, Y. Determination of Hydrogen Peroxide in Fish Products and Noodles (Japanese) by GasLiquid Chromatography with Electron-Capture Detection. *J. Agric. Food Chem.* **1990**, *38* (12), 2154–2159. https://doi.org/10.1021/jf00102a011.

(15) Wu, P.; Qian, Y.; Du, P.; Zhang, H.; Cai, C. Facile Synthesis of Nitrogen-Doped Graphene for Measuring the Releasing Process of Hydrogen Peroxide from Living Cells. *J. Mater. Chem.* **2012**, *22* (13), 6402–6412. https://DOI: 10.1039/c2jm16929k

(16) Kojima, H.; Nakatsubo, N.; Kikuchi, K.; Kawahara, S.; Kirino, Y.; Nagoshi, H.; Hirata, Y.; Nagano, T. Detection and Imaging of Nitric Oxide with Novel Fluorescent Indicators: Diaminofluoresceins. *Anal. Chem.* **1998**, *70* (13), 2446–2453. https://doi.org/10.1021/ac9801723.
(17) Li, C.; Zhang, H.; Wu, P.; Gong, Z.; Xu, G.; Cai, C. Electrochemical Detection of Extracellular Hydrogen Peroxide Released from RAW 264.7 Murine Macrophage Cells Based on Horseradish Peroxidase-Hydroxyapatite Nanohybrids. *Analyst* **2011**, *136* (6), 1116–1123. https://doi.org/10.1039/c0an00825g.
(18) Wang, J.; Li, L.; Huang, W.; Cheng, J. Development and Evaluation of a Rotary Cell for Capillary Electrophoresis-Chemiluminescence Detection. *Anal. Chem.* **2010**, *82* (12), 5380–5383. https://doi.org/10.1021/ac100007d.
(19) Bartosz, G. Use of Spectroscopic Probes for Detection of Reactive Oxygen Species. *Clin. Chim. Acta* **2006**, *368* (1–2), 53–76. https://doi.org/10.1016/j.cca.2005.12.039.
(20) Wu, P.; Cai, Z.; Gao, Y.; Zhang, H.; Cai, C. Enhancing the Electrochemical Reduction of Hydrogen Peroxide Based on Nitrogen-Doped Graphene for Measurement of Its Releasing Process from Living Cells. *Chem. Commun.* **2011**, *47* (40), 11327–11329. https://doi.org/10.1039/c1cc14419g.
(21) Wang, Y.; Shao, Y.; Matson, D. W.; Li, J.; Lin, Y. Nitrogen-Doped Graphene and Its Application in Electrochemilal Biosensing. *J. Nanosci. Nanotechnol.* **2010**, *4* (4), 1790–1798 ▪. https://doi.org/10.1021/nn100315s.
(22) Cui, R.; Han, Z.; Pan, J.; Abdel-Halim, E. S.; Zhu, J. J. Direct Electrochemistry of Glucose Oxidase and Biosensing for Glucose Based on Helical Carbon Nanotubes Modified Magnetic Electrodes. *Electrochim. Acta* **2011**, *58* (1), 179–183. https://doi.org/10.1016/j.electacta.2011.09.030.
(23) Juska, V. B.; Pemble, M. E. A Critical Review of Electrochemical Glucose Sensing: Evolution of Biosensor Platforms Based on Advanced Nanosystems. *Sensors (Switzerland)* **2020**, *20* (21), 1–28. https://doi.org/10.3390/s20216013.
(24) Zheng, Y. L.; Mei, D.; Chen, Y. X.; Ye, S. The Redox Reaction of Hydrogen Peroxide at an Au(100) Electrode: Implications for Oxygen Reduction Kinetics. *Electrochem. commun.* **2014**, *39*, 19–21. https://doi.org/10.1016/j.elecom.2013.12.005.
(25) Gulaboski, R.; Mirčeski, V.; Kappl, R.; Hoth, M.; Bozem, M. Review—Quantification of Hydrogen Peroxide by Electrochemical Methods and Electron Spin Resonance Spectroscopy. *J. Electrochem. Soc.* **2019**, *166* (8), G82–G101. https://doi.org/10.1149/2.1061908jes.
(26) González-Sánchez, M. I.; Gómez-Monedero, B.; Agrisuelas, J.; Iniesta, J.; Valero, E. Highly Activated Screen-Printed Carbon Electrodes by Electrochemical Treatment with Hydrogen Peroxide. *Electrochem. commun.* **2018**, *91* (May), 36–40. https://doi.org/10.1016/j.elecom.2018.05.002.
(27) Wang, S. C.; Chang, K. S.; Yuan, C. J. Enhancement of Electrochemical Properties of Screen-Printed Carbon Electrodes by Oxygen Plasma Treatment. *Electrochim. Acta* **2009**, *54* (21), 4937–4943. https://doi.org/10.1016/j.electacta.2009.04.006.
(28) Karyakin, A. A. Prussian Blue and Its Analogues: Electrochemistry and Analytical Applications Arkady. *Electroanalysis* **2001**, *13* (10), 813–819.
(29) Ricci, F.; Amine, A.; Palleschi, G.; Moscone, D. Prussian Blue Based Screen Printed Biosensors with Improved Characteristics of Long-Term Lifetime and PH Stability. *Biosens. Bioelectron.* **2002**, *18* (2–3), 165–174.

(30) Du, D.; Wang, M.; Qin, Y.; Lin, Y. One-Step Electrochemical Deposition of Prussian Blue-Multiwalled Carbon Nanotube Nanocomposite Thin-Film: Preparation, Characterization and Evaluation for H2O2 Sensing. *J. Mater. Chem.* **2010**, *20* (8), 1532–1537. https://doi.org/10.1039/b919500a.
(31) Zhang, W.; Wang, L.; Zhang, N.; Wang, G.; Fang, B. Functionalization of Single-Walled Carbon Nanotubes with Cubic Prussian Blue and Its Application for Amperometric Sensing. *Electroanalysis* **2009**, *21* (21), 2325–2330. https://doi.org/10.1002/elan.200904690.
(32) Kumar, S. M. S.; Pillai, K. C. Compositional Changes in Unusually Stabilized Prussian Blue by CTAB Surfactant: Application to Electrocatalytic Reduction of H2O 2. *Electrochem. commun.* **2006**, *8* (4), 621–626. https://doi.org/10.1016/j.elecom.2006.02.009.
(33) Moscone, D.; D'Ottavi, D.; Compagnone, D.; Palleschi, G.; Amine, A. Construction and Analytical Characterization of Prussian Blue-Based Carbon Paste Electrodes and Their Assembly as Oxidase Enzyme Sensors. *Anal. Chem.* **2001**, *73* (11), 2529–2535. https://doi.org/10.1021/ac001245x.
(34) Agrisuelas, J.; González-Sánchez, M. I.; Valero, E. Hydrogen Peroxide Sensor Based on in Situ Grown Pt Nanoparticles from Waste Screen-Printed Electrodes. *Sensors Actuators, B Chem.* **2017**, *249*, 499–505. https://doi.org/10.1016/j.snb.2017.04.136.
(35) Chikae, M.; Idegami, K.; Kerman, K.; Nagatani, N.; Ishikawa, M.; Takamura, Y.; Tamiya, E. Direct Fabrication of Catalytic Metal Nanoparticles onto the Surface of a Screen-Printed Carbon Electrode. *Electrochem. commun.* **2006**, *8* (8), 1375–1380. https://doi.org/10.1016/j.elecom.2006.06.019.
(36) Tangkuaram, T.; Ponchio, C.; Kangkasomboon, T.; Katikawong, P.; Veerasai, W. Design and Development of a Highly Stable Hydrogen Peroxide Biosensor on Screen Printed Carbon Electrode Based on Horseradish Peroxidase Bound with Gold Nanoparticles in the Matrix of Chitosan. *Biosens. Bioelectron.* **2007**, *22* (9–10), 2071–2078. https://doi.org/10.1016/j.bios.2006.09.011.
(37) Teng, Y. J.; Zuo, S. H.; Lan, M. B. Direct Electron Transfer of Horseradish Peroxidase on Porous Structure of Screen-Printed Electrode. *Biosens. Bioelectron.* **2009**, *24* (5), 1353–1357. https://doi.org/10.1016/j.bios.2008.07.062.
(38) Ledru, S.; Ruillé, N.; Boujtita, M. One-Step Screen-Printed Electrode Modified in Its Bulk with HRP Based on Direct Electron Transfer for Hydrogen Peroxide Detection in Flow Injection Mode. *Biosens. Bioelectron.* **2006**, *21* (8), 1591–1598. https://doi.org/10.1016/j.bios.2005.07.020.
(39) Buk, V.; Emregul, E.; Emregul, K. C. Alginate Copper Oxide Nano-Biocomposite as a Novel Material for Amperometric Glucose Biosensing. *Mater. Sci. Eng. C* **2017**, *74*, 307–314. https://doi.org/10.1016/j.msec.2016.12.003.
(40) Shan, C.; Yang, H.; Han, D.; Zhang, Q.; Ivaska, A.; Niu, L. Graphene/AuNPs/Chitosan Nanocomposites Film for Glucose Biosensing. *Biosens. Bioelectron.* **2010**, *25* (5), 1070–1074. https://doi.org/10.1016/j.bios.2009.09.024.
(41) Yuan, Y.; Wang, Y.; Wang, H.; Hou, S. Gold Nanoparticles Decorated on Single Layer Graphene Applied for Electrochemical Ultrasensitive Glucose Biosensor. *J. Electroanal. Chem.* **2019**, *855* (November 2018), 113495. https://doi.org/10.1016/j.jelechem.2019.113495.
(42) Razmi, H.; Mohammad-Rezaei, R. Graphene Quantum Dots as a New Substrate for

Immobilization and Direct Electrochemistry of Glucose Oxidase: Application to Sensitive Glucose Determination. *Biosens. Bioelectron.* **2013**, *41* (1), 498–504. https://doi.org/10.1016/j.bios.2012.09.009.

(43) Buk, V.; Pemble, M. E. A Highly Sensitive Glucose Biosensor Based on a Micro Disk Array Electrode Design Modified with Carbon Quantum Dots and Gold Nanoparticles. *Electrochim. Acta* **2019**, *298*, 97–105. https://doi.org/10.1016/j.electacta.2018.12.068.

(44) Lin, Y.; Lu, F.; Tu, Y.; Ren, Z. Glucose Biosensors Based on Carbon Nanotube Nanoelectrode Ensembles. *Nano Lett.* **2004**, *4* (2), 191–195. https://doi.org/10.1021/nl0347233.

(45) Xu, S.; Zhang, Y.; Zhu, Y.; Wu, J.; Li, K.; Lin, G.; Li, X.; Liu, R.; Liu, X.; Wong, C. P. Facile One-Step Fabrication of Glucose Oxidase Loaded Polymeric Nanoparticles Decorating MWCNTs for Constructing Glucose Biosensing Platform: Structure Matters. *Biosens. Bioelectron.* **2019**, *135* (March), 153–159. https://doi.org/10.1016/j.bios.2019.04.017.

(46) Yu, Y.; Chen, Z.; He, S.; Zhang, B.; Li, X.; Yao, M. Direct Electron Transfer of Glucose Oxidase and Biosensing for Glucose Based on PDDA-Capped Gold Nanoparticle Modified Graphene/Multi-Walled Carbon Nanotubes Electrode. *Biosens. Bioelectron.* **2014**, *52*, 147–152. https://doi.org/10.1016/j.bios.2013.08.043.

(47) Fanjul-Bolado, P.; Queipo, P.; Lamas-Ardisana, P. J.; Costa-García, A. Manufacture and Evaluation of Carbon Nanotube Modified Screen-Printed Electrodes as Electrochemical Tools. *Talanta* **2007**, *74* (3), 427–433. https://doi.org/10.1016/j.talanta.2007.07.035.

(48) Shi, L.; Niu, X.; Liu, T.; Zhao, H.; Lan, M. Electrocatalytic Sensing of Hydrogen Peroxide Using a Screen Printed Carbon Electrode Modified with Nitrogen-Doped Graphene Nanoribbons. *Microchim. Acta* **2015**, *182* (15–16), 2485–2493. https://doi.org/10.1007/s00604-015-1605-6.

(49) Maldonado, S.; Stevenson, K. J. Direct Preparation of Carbon Nanofiber Electrodes via Pyrolysis of Iron(II) Phthalocyanine: Electrocatalytic Aspects for Oxygen Reduction. *J. Phys. Chem. B* **2004**, *108* (31), 11375–11383. https://doi.org/10.1021/jp0496553.

(50) Liu, B.; Yao, H.; Song, W.; Jin, L.; Mosa, I. M.; Rusling, J. F.; Suib, S. L.; He, J. Ligand-Free Noble Metal Nanocluster Catalysts on Carbon Supports via "Soft" Nitriding. *J. Am. Chem. Soc.* **2016**, *138* (14), 4718–4721. https://doi.org/10.1021/jacs.6b01702.

(51) Xu, X.; Yuan, T.; Zhou, Y.; Li, Y.; Lu, J.; Tian, X.; Wang, D.; Wang, J. Facile Synthesis of Boron and Nitrogen-Doped Graphene as Efficient Electrocatalyst for the Oxygen Reduction Reaction in Alkaline Media. *Int. J. Hydrogen Energy* **2014**, *39* (28), 16043–16052. https://doi.org/10.1016/j.ijhydene.2013.12.079.

(52) Mou, Z.; Chen, X.; Du, Y.; Wang, X.; Yang, P.; Wang, S. Forming Mechanism of Nitrogen Doped Graphene Prepared by Thermal Solid-State Reaction of Graphite Oxide and Urea. *Appl. Surf. Sci.* **2011**, *258* (5), 1704–1710. https://doi.org/10.1016/j.apsusc.2011.10.019.

(53) Shao, Y.; Zhang, S.; Engelhard, M. H.; Li, G.; Shao, G.; Wang, Y.; Liu, J.; Aksay, I. A.; Lin, Y. Nitrogen-Doped Graphene and Its Electrochemical Applications. *J. Mater. Chem.* **2010**, *20* (35), 7491–7496. https:// DOI: 10.1039/C0JM00782J.

(54) Lyu, Y. P.; Wu, Y. S.; Wang, T. P.; Lee, C. L.; Chung, M. Y.; Lo, C. T. Hydrothermal and Plasma Nitrided Electrospun Carbon Nanofibers for Amperometric Sensing of Hydrogen Peroxide. *Microchim. Acta* **2018**, *185* (8), 3–9. https://doi.org/10.1007/s00604-018-2915-2.

(55) Wu, P.; Du, P.; Zhang, H.; Cai, C. Microscopic Effects of the Bonding Configuration of Nitrogen-Doped Graphene on Its Reactivity toward Hydrogen Peroxide Reduction Reaction. *Phys. Chem. Chem. Phys.* **2013**, *15* (18), 6920–6928. https://doi.org/10.1039/c3cp50900a.

(56) Liu, B.; Yao, H.; Song, W.; Jin, L.; Mosa, I. M.; Rusling, J. F.; Suib, S. L.; He, J. Ligand-Free Noble Metal Nanocluster Catalysts on Carbon Supports via " Soft " Nitriding. **2016**. https://doi.org/10.1021/jacs.6b01702.

(57) Liu, B.; Yao, H.; Song, W.; Jin, L.; Mosa, I. M.; James, F.; Suib, S. L.; He, J.; States, U.; Emulsions, G.; States, U.; States, U. Ligand-Free Noble Metal Nanocluster Catalysts on Carbon Supports via "Soft" Nitriding. *J Am Chem Soc* **2017**, *138* (14), 4718–4721. https://doi.org/10.1021/jacs.6b01702.Synthetic.

(58) Ogbu, C. I.; Feng, X.; Dada, S. N.; Bishop, G. W. Screen-Printed Soft-Nitrided Carbon Electrodes for Detection of Hydrogen Peroxide. *Sensors (Switzerland)* **2019**, *19* (17), 1–16. https://doi.org/10.3390/s19173741.

(59) Bishop, G. W.; Ahiadu, B. K.; Smith, J. L.; Patterson, J. D. Use of Redox Probes for Characterization of Layer-by-Layer Gold Nanoparticle-Modified Screen-Printed Carbon Electrodes. *J. Electrochem. Soc.* **2017**, *164* (2), B23–B28. https://doi.org/10.1149/2.0431702jes.

(60) Elgrishi, N.; Rountree, K. J.; McCarthy, B. D.; Rountree, E. S.; Eisenhart, T. T.; Dempsey, J. L. A Practical Beginner's Guide to Cyclic Voltammetry. *J. Chem. Educ.* **2018**, *95* (2), 197–206. https://doi.org/10.1021/acs.jchemed.7b00361.

(61) Cumba, L. R.; Foster, C. W.; Brownson, D. A. C.; Smith, J. P.; Iniesta, J.; Thakur, B.; Do Carmo, D. R.; Banks, C. E. Can the Mechanical Activation (Polishing) of Screen-Printed Electrodes Enhance Their Electroanalytical Response? *Analyst* **2016**, *141* (9), 2791–2799. https://doi.org/10.1039/c6an00167j.

(62) Randviir, E. P.; Brownson, D. A. C.; Metters, J. P.; Kadara, R. O.; Banks, C. E. The Fabrication, Characterisation and Electrochemical Investigation of Screen-Printed Graphene Electrodes. *Phys. Chem. Chem. Phys.* **2014**, *16* (10), 4598–4611. https://doi.org/10.1039/c3cp55435j.

(63) Wang, Y.; Shao, Y.; Matson, D. W.; Li, J.; Lin, Y. Nitrogen-Doped Graphene and Its Biosensing. *ACS Nano* **2010**, *4* (4), 1790–1798. https://doi.org/10.1063/1.4870424.

(64) Kadara, R. O.; Jenkinson, N.; Banks, C. E. Characterisation of Commercially Available Electrochemical Sensing Platforms. *Sensors Actuators, B Chem.* **2009**, *138* (2), 556–562. https://doi.org/10.1016/j.snb.2009.01.044.

(65) Reanpang, P.; Themsirimongkon, S.; Saipanya, S.; Chailapakul, O.; Jakmunee, J. Cost-Effective Flow Injection Amperometric System with Metal Nanoparticle Loaded Carbon Nanotube Modified Screen Printed Carbon Electrode for Sensitive Determination of Hydrogen Peroxide. *Talanta* **2015**, *144*, 868–874. https://doi.org/10.1016/j.talanta.2015.07.041.

(66) Elewi, A. S.; Al-Shammaree, S. A. W.; AL Sammarraie, A. K. M. A. Hydrogen Peroxide Biosensor Based on Hemoglobin-Modified Gold Nanoparticles–Screen Printed Carbon Electrode. *Sensing and Bio-Sensing Research*. 2020. https://doi.org/10.1016/j.sbsr.2020.100340.

(67) Li, G.; Wang, Y.; Xu, H. A Hydrogen Peroxide Sensor Prepared by Electropolymerization of Pyrrole Based on Screen-Printed Carbon Paste Electrodes. *Sensors* **2007**, *7* (3), 239–250. https://doi.org/10.3390/s7030239.

(68) Zen, J. M.; Chung, H. H.; Kumar, A. S. Flow Injection Analysis of Hydrogen Peroxide on Copper-Plated Screen-Printed Carbon Electrodes. *Analyst* **2000**, *125* (9), 1633–1637. https://doi.org/10.1039/b004207m.
(69) Lee, S.; Lee, Y. J.; Kim, J. H.; Lee, G. J. Electrochemical Detection of H2O2 Released from Prostate Cancer Cells Using Pt Nanoparticle-Decorated RGO-CNT Nanocomposite-Modified Screen-Printed Carbon Electrodes. *Chemosensors* **2020**, *8* (3). https://doi.org/10.3390/CHEMOSENSORS8030063.

VITA

EMMANUEL NKYAAGYE

Education:

B.S (Hons). Chemistry, University of Cape Coast, Cape Coast, Ghana, 2018

M.S. Chemistry, East Tennessee State University, Johnson City, Tennessee, 2021

Professional Experience:

Teaching Assistant, Department of Chemistry, University of Cape Coast, Cape Coast, Ghana,
September 2018 - December 2019

Graduate Teaching Assistant, Department of Chemistry, East Tennessee State University,
January 2020 – December 2021

Research Assistant, Department of Chemistry, East Tennessee State University,
(Mentor: Dr Gregory W. Bishop)
January 2020 – December 2021

Research Experience:

Undergraduate Research Student, University of Cape – Coast,
Cape – Coast, Ghana
2017 – 2018
(Mentor: Dr Francis Nsiah)
Use of Silver Nanoparticles as Iron Contaminant Removal Media in Selected Water Samples in the Cape Coast Metropolis.

Research Assistant, Department of Chemistry, East Tennessee State University,
(Mentor: Dr Gregory W. Bishop)
2020 – 2021
Facile Nitrogen-Doping of Screen-Printed Carbon Electrodes for Detection of Hydrogen Peroxide